

## SPATIAL AND TEMPORAL INVARIANCE IN THE SPECTRA OF ENERGETIC PARTICLES IN GRADUAL SOLAR EVENTS

D. V. REAMES

NASA/Goddard Space Flight Center, Greenbelt, MD 20771; reames@lheavx.gsfc.nasa.gov

S. W. KAHLER

Phillips Laboratory/GPSG, 29 Randolph Road, Hanscom AFB, MA 01731-3010; kahler@plh.af.mil

AND

C. K. NG

Department of Mathematics, Royal Melbourne Institute of Technology, Melbourne 3001, Australia; chee.ng@rmit.edu.au

Received 1997 April 7; accepted 1997 July 16

### ABSTRACT

We show evidence of spatial and temporal invariance in the energy spectra of  $\sim 1$ –100 MeV protons from large gradual solar energetic particle (SEP) events. Nearly identical spectra are seen over longitude intervals of up to  $160^\circ$ , and the intensities at all energies decline with  $e$ -folding time constants of 6–18 hr for periods of  $\sim 3$  days. The region of the invariant spectra is associated with acceleration on the eastern flank of the shock wave driven out from the Sun by a coronal-mass ejection (CME). The quasi-parallel shock in this region changes only slowly with time, and a quasi equilibrium is established for particles stored on field lines in the expanding volume between the shock and the Sun. On the western flank of the shock, the SEP event is more dynamic. Here, the nearly quasi-perpendicular shock produces harder spectra that change more rapidly with time as regions of the shock with varying speed and angle sweep across the observer's field line.

Gradual SEP events arise from large CMEs with sufficient speeds to generate shocks that are fast enough to accelerate particles. In our study, shocks with transit speed  $> 750 \text{ km s}^{-1}$  always accelerate particles, while those with speeds of  $500$ – $750 \text{ km s}^{-1}$  sometimes do. However, invariant spectra seem to occur in all gradual SEP events as a consequence of the structure and topology of the CME and shock.

*Subject headings:* acceleration of particles — shock waves — Sun: corona — Sun: particle emission

### 1. INTRODUCTION

In recent years it has become clear that energetic particles observed in the large “gradual” solar energetic particle (SEP) events are accelerated at shock waves driven out of the corona by coronal mass ejections (CMEs) and not in solar flares (see reviews by Reames 1990, 1993, 1995a, Kahler 1992; Gosling 1993). Many years ago, Kahler et al. (1984) found a 96% correlation between large SEP events and CMEs and a correlation between SEP intensities and the size and speed of the CME. Since that time, evidence about the spatial and temporal distributions of the particles (see Reames 1993, 1995a), as well as about their abundances (Mason, Gloeckler, & Hovestadt 1984; Cane, McGuire, & von Roseninge 1986; Reames & Stone 1986; Reames 1995b) and charge states (Luhn et al. 1984, 1987; Leske et al. 1995; Mason et al. 1995; Tylka et al. 1995; Oetliker et al. 1997), has strengthened the association between SEP events and large, fast CMEs. For example, recent evidence on the ionization of energetic Fe ions at energies as high as  $200$ – $600 \text{ MeV amu}^{-1}$  shows them to have charge  $14.1 \pm 1.4$  (Tylka et al. 1995), indicating that these ions were accelerated from ambient coronal material at a temperature of  $\sim 2$  MK. Not only could they not have come from the hot material in a flare, but they would be stripped of electrons in seconds at the densities of the low corona and could not be accelerated or stored in or around flare loops. Kahler (1994) has shown that protons up to 21 GeV are accelerated with highest efficiency at a distance of 5–10 solar radii where densities are much lower.

The large spatial extent of SEP events has been known for many years (e.g., McKibben 1972), but the first associ-

ation of the particle time profiles with the longitude and structure of the evolving shock was made by Cane, Reames, & von Roseninge (1988). More recently, Reames, Barbier, & Ng (1996; hereafter RBN 1996) performed a detailed multispacecraft study of the spatial structure of these large SEP events relative to that of the CME-driven shock.

Generally speaking, it is known that particle energy spectra can vary widely in SEP events, both in space and time (see RBN 1996). However, two recent lines of evidence have suggested the possibility of a large spatial region where spectral shapes are constant in space and time, extending the original discovery of this invariance by McKibben (1972). First RBN (1996) found large regions behind the shocks and CMEs where the proton intensities at widely separated spacecraft were nearly identical and declined together in time. They described an expanding region of quasi-trapped particles between the shock and the Sun where intensities gradually decline from adiabatic deceleration, which preserves spectral shape, as the particles do work on the expanding magnetic “bottle” that contains them. Second, Reames et al. (1997) found that the intensities of He and other ions with energies above  $34 \text{ keV amu}^{-1}$  had nearly identical temporal behavior for a 3 day period during the 1995 October 20 event from a source at  $W55^\circ$ . Such detailed spectral invariance, both before and after shock passage, covering orders of magnitude in energy, was indeed surprising.

In this paper, we return to the extensive historic data base provided by the *IMP 8* and *Helios 1* and *2* spacecraft to search for the origin of spatial and temporal invariance in the large SEP events.

## 2. SPATIAL INVARIANCE OF SPECTRA

Among the events studied by RBN (1996) were several with three spacecraft favorably located to sample the SEP distributions over a wide region of space. One of the most impressive of these events was that of 1978 September 23. During this large event, the shock itself was seen by all three spacecraft distributed over  $160^\circ$  in solar longitude as shown in the inset in Figure 1. In this inset and all others, the CME is presumed to be directed downward and is indicated by the longitude of the accompanying flare (as observed from Earth), since CME longitudes are not directly measured. Despite data gaps, the time profiles of 3–6 MeV protons in the upper panel of Figure 1 show the common feature that the intensities at all three spacecraft join to follow a common curve, within a factor of  $\sim 2$ , late in the event. Complete proton-energy spectra have been taken during

the intervals labeled A and B, where data from all three spacecraft are available. These spectra are shown in the lower panels of the figure. During period A, spectra at the three spacecraft show very different intensities at all energies. In contrast, during period B, the spectra from all three spacecraft are in excellent agreement despite the wide separation of the spacecraft.

A second example from RBN (1996), where the three spacecraft had complete coverage of a somewhat smaller SEP event, is the 1979 March 1 event shown in Figure 2. Here again, spectra are shown for a period A early in the event and a period B that occurs immediately after the 3–6 MeV proton intensities at the three spacecraft join on March 5. Again there are sharp differences in the spectra during the early period and similarities in those taken late in the event. During the decay phase of the event, the intensity at *IMP 8* is about a factor of 2 higher than at the other

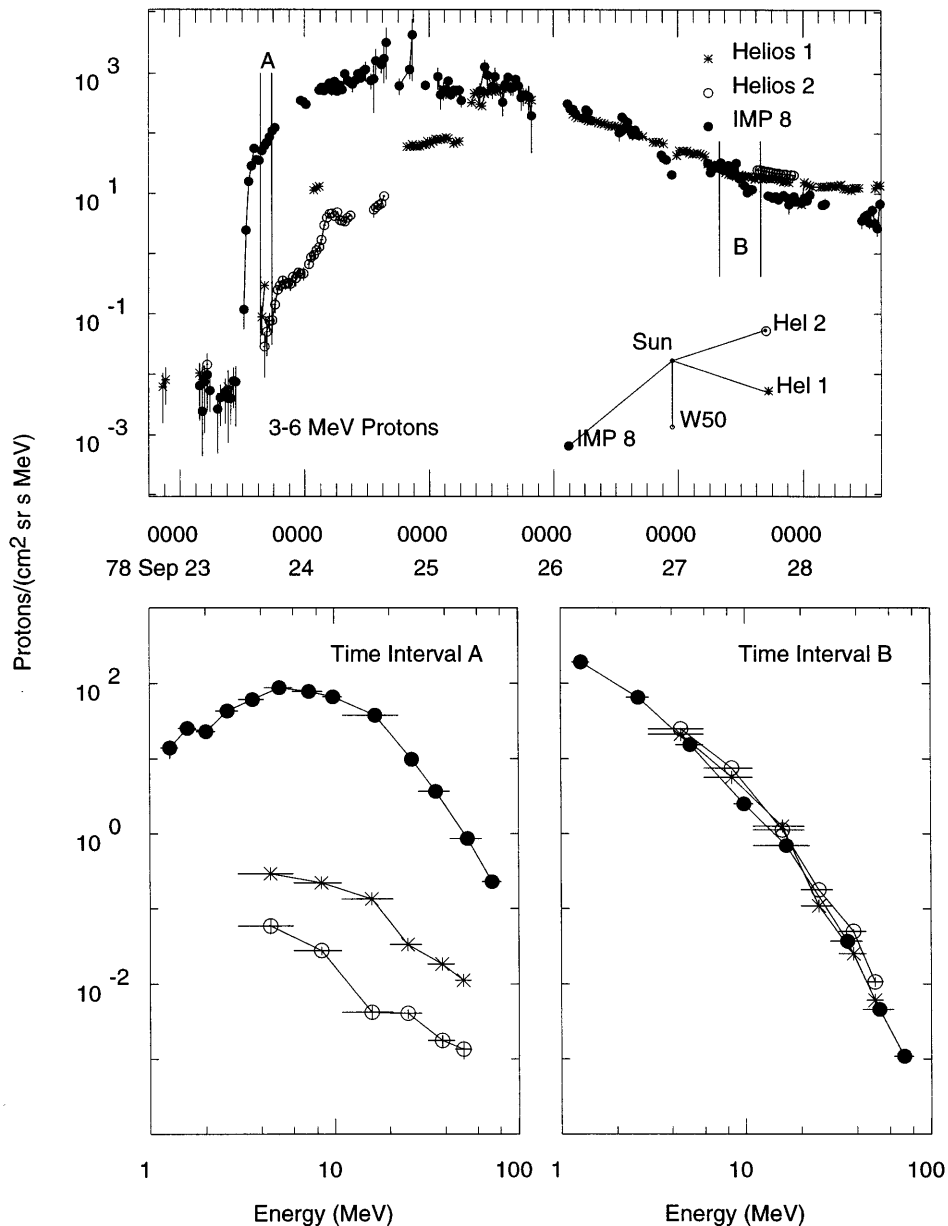


FIG. 1.—Time-intensity profiles are shown in the upper panel for 3–6 MeV protons observed during the 1978 September 23 SEP event by *Helios 1*, *Helios 2*, and *IMP 8* for the spacecraft positions shown in the inset. Spectra taken at the three spacecraft during time periods marked A and B are shown in the lower panels.

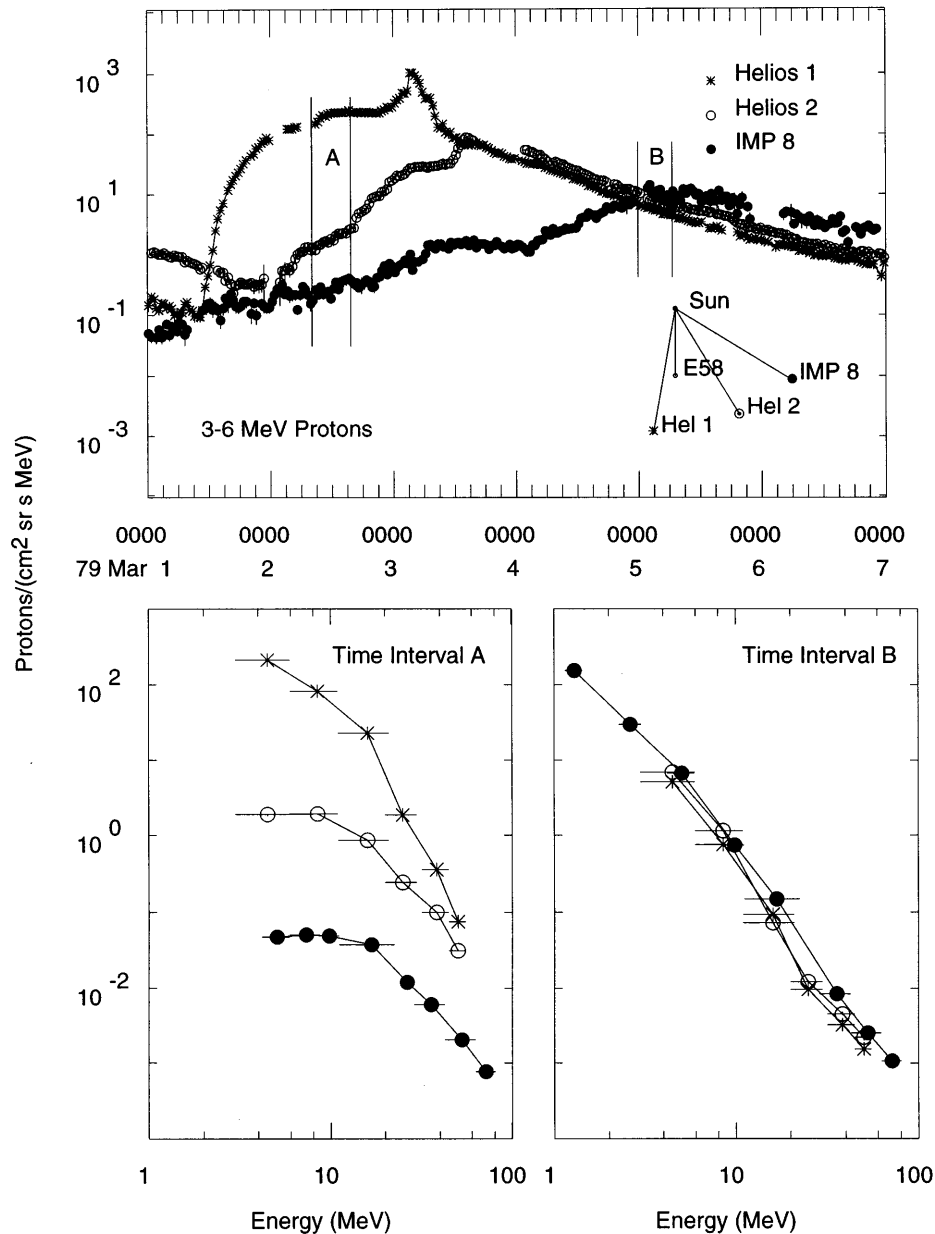


FIG. 2.—Time-intensity profiles are shown in the upper panel for 3–6 MeV protons observed during the 1979 March 1 SEP event by *Helios 1*, *Helios 2*, and *IMP 8* for the spacecraft positions shown in the inset. Spectra taken at the three spacecraft during time periods marked A and B are shown in the lower panels.

two spacecraft. It is likely that, by this late time in the event, solar rotation has carried field lines with the greatest intensities westward in the direction of *IMP 8*. When these small intensity differences do exist late in these events, the spacecraft connected farthest east from the nose of the shock sees the lowest intensity. The near equality of the spectra to within a factor  $\sim 2$  at spacecraft widely separated in longitude implies that corotation has negligible effect on intensity decay. At such times, the observed intensity decay at any spacecraft reflects the intrinsic intensity decay in a corotating interplanetary flux tube.

At late times in both of the events we have examined, it is clear that the similar intensities of 3–6 MeV protons seen at widely separated spacecraft are not the coincidental merging of intensities in a limited energy region; they apply to the entire spectral region we are able to observe.

### 3. TIME-INVARIANT SPECTRA

Not only can the spectra be similar at widely separated spatial points, as shown in the previous section, but those spectral shapes are maintained for time periods of several days as the shock expands and the overall level of the intensity declines.

Figure 3 shows the time-intensity profiles for the 1978 September 23 event normalized on September 27 by dividing the intensity at each energy by the corresponding value on the spectra taken during period B in Figure 1. Data for *Helios 2* are not shown because of the extensive data gaps for that spacecraft. A short time after shock passage, we see at the locations of both *Helios 1* and *IMP 8* that the intensities at all energies merge to follow a similar curve for a period of  $\sim 3$  days. Note the sudden onset of this invariant region at *Helios 1*; prior to this onset, much harder spectra

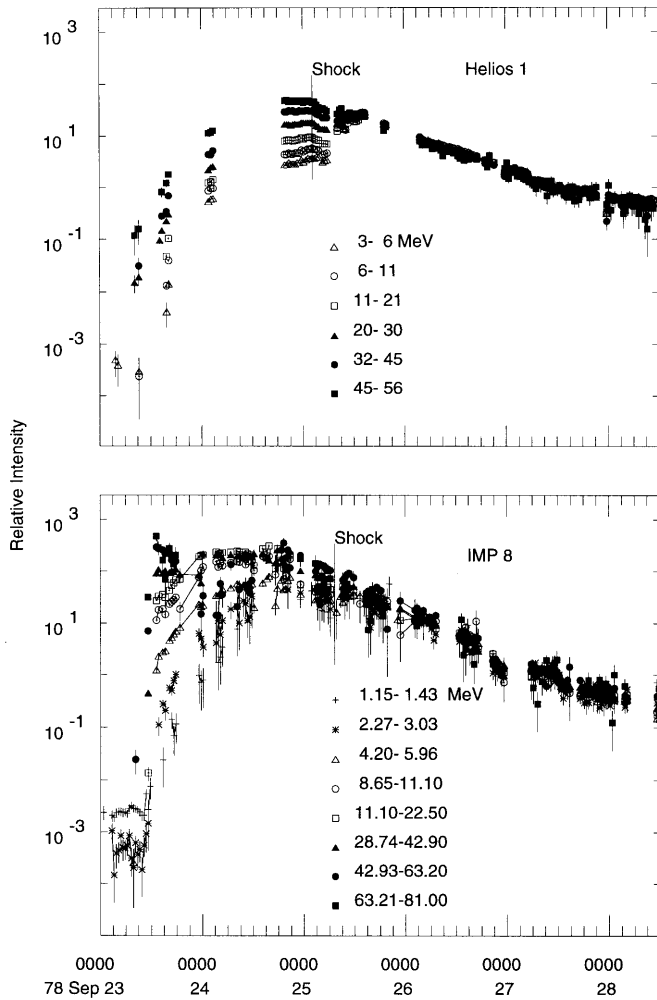


FIG. 3.—Time-intensity profiles at the proton energies shown for *Helios 1* and *IMP 8* during the 1978 September 23 SEP event. The intensity at each energy is normalized by the value obtained during time period B on September 27 and shown in the spectrum in Fig. 1.

were observed. We should also note that it is likely that detectors on *IMP 8* were saturated from about 1800 UT on September 23 until about 1800 UT on September 24.

Figure 4 shows the intensities at different energies for the 1979 March 1 event normalized by the spectra taken during period B shown in Figure 2. Here the spectra for *Helios 1* and *2* seem to depart from invariance late in the event. However, this apparent departure occurs because the higher energy protons are returning to instrument background, not because the SEP spectra are hardening late in the event. The more sensitive instrument on *IMP 8* shows time-invariant spectra between 1 and 60 MeV for a period of  $\sim 3$  days. The onset of this invariance occurs rather abruptly at *IMP 8*. Early in the event, the spectra are much harder at all three spacecraft, but the shock has certainly weakened by the time it passes *Helios 1*, and the spectra have softened as described in RBN (1996).

Figure 5 shows normalized *Helios 1* and *IMP 8* time profiles for the 1981 May 16 event. The CME and the shock from this event were discussed by both Kahler et al. (1984) and Sheeley et al. (1985). *Helios 1*, at a distance of 0.59 AU, sees a shock transit speed of  $1790 \text{ km s}^{-1}$ , while *IMP 8*, apparently more directly in line with the CME, has a shock transit speed of only  $1050 \text{ km s}^{-1}$ . This seems to be a clear

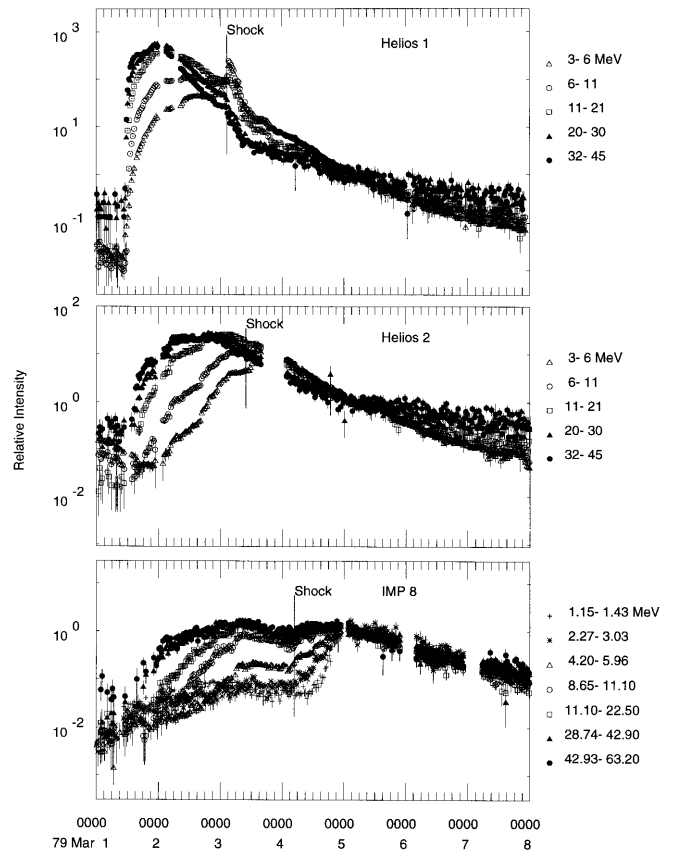


FIG. 4.—Time-intensity profiles at the proton energies shown for *Helios 1*, *Helios 2*, and *IMP 8* during the 1979 March 1 SEP event. The intensity at each energy is normalized by the value obtained during time period B on March 5 and shown in the spectrum in Fig. 2.

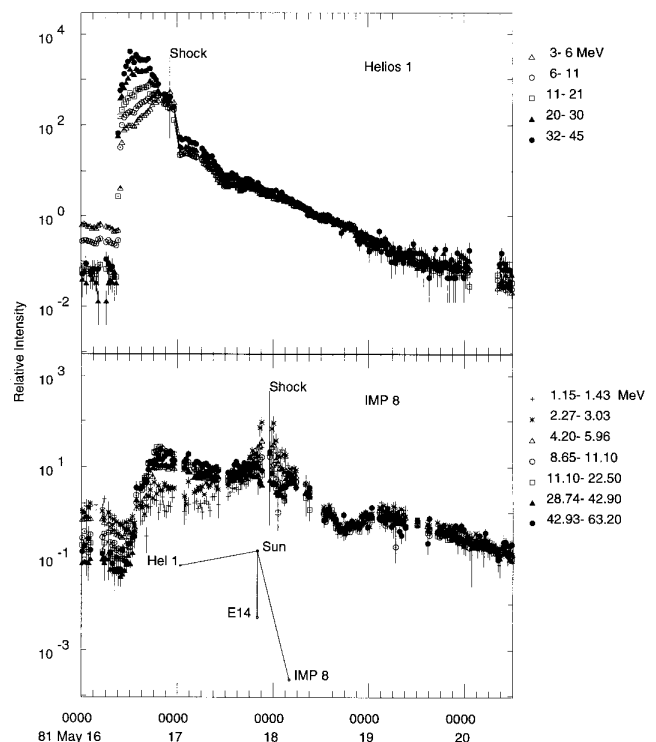


FIG. 5.—Normalized time-intensity profiles for the proton energies shown for *Helios 1* and *IMP 8* during the 1981 May 16 SEP event. The spacecraft configuration during this event is shown in the inset.

case in which the central longitudes of the CME and the flare do not coincide well and in which the shock speed varies strongly with longitude. The period of spectral invariance begins abruptly just before shock passage at *Helios 1* and lasts several days. At *IMP 8*, spectral invariance begins several hours after shock passage.

Unfortunately, not all events can be observed by multiple spacecraft. Figure 6 shows intensity profiles for the 1980 November 14 event observed nearly head-on 0.51 AU from the Sun by *Helios 1*. The shock transit speed was  $1510 \text{ km s}^{-1}$  (Sheeley et al. 1985). An invariant period of several days is seen after shock passage for this event. Note particularly that during the shock passage, at time B, the spectrum is much harder than it is either before (time A) or afterward (time C). This is an event in which the spacecraft seems to pass directly through the strongest acceleration region near the nose of an active shock where the hardest spectra are found. Here, the intensities at all energies peak within one time-averaging interval (30 minutes) of the shock. Usually, spacecraft will pass to the east (or west) of the shock nose so that intensities peak before (or after) shock passage, when field lines are best connected to the nose of the shock. Also in this event, it is clear that the shock is still actively accel-

ating particles out to energies of at least 60 MeV. This differs from the situation in the 1979 March 1 event (Fig. 4, upper panel) where only the lowest energies still peak near the shock at *Helios 1*; this shock no longer actively accelerates higher energy particles where the spacecraft crosses it.

#### 4. EVENT STATISTICS

In order to determine how frequently invariant spectra occur in CME events, we have examined particle data in all of the 56 CME/shock events studied by Sheeley et al. (1985) when *Helios 1* was likely to be favorably located off the east or west limbs of the Sun and when CME observations were made by the *Solwind* coronagraph in Earth orbit. This event list was produced by associating CMEs and interplanetary shocks; it is completely unbiased with respect to SEPs since they were not considered at all. The presence or absence of SEP events cannot be determined in 27 cases because of data gaps (15 cases), high background in the experiment (seven cases), and confusion of multiple events (five cases). Of the remaining 29 events, 21 had clearly associated SEP events, while eight had no evidence of a particle increase at *Helios 1*. Properties of the 29 events are shown in Table 1. Columns in the table give the onset time of the CME or associated flare (if any), the speed and angular span of the CME, the average (transit) speed of the shock, the shock speed at *Helios 1*, the radial position and longitude of *Helios 1*, the flare longitude (if any) relative to Earth and to *Helios 1*, the peak intensity of 3–6 MeV protons in units of  $(\text{cm}^2 \text{ sr s MeV})^{-1}$ , and the  $e$ -folding decay time in the invariant region. Most CME and shock properties are taken from Sheeley et al. (1985).

It is interesting that the mean shock transit speed of the events without SEPs is  $560 \text{ km s}^{-1}$ , while that of events with SEPs is  $987 \text{ km s}^{-1}$ . The greatest shock transit speed for the events without particles is listed in Sheeley et al. (1985) as  $750 \text{ km s}^{-1}$  (followed by a question mark); 14 of the 21 events with SEPs have transit speeds that exceed  $750 \text{ km s}^{-1}$ . Thus, all events with speeds  $>750 \text{ km s}^{-1}$  have associated SEPs, while events with speeds  $500\text{--}750 \text{ km s}^{-1}$  occasionally do and those with speeds  $<500 \text{ km s}^{-1}$  have no SEP association. The events with SEPs show a similar correlation between speed and particle intensity to that previously reported by Kahler et al. (1984). In addition, these results are in substantial agreement with those of Kahler et al. (1987), who found that 29 of 31 fast CMEs, with speeds  $>800 \text{ km s}^{-1}$ , had associated SEP events. Furthermore, shock transit speeds can be determined for 119 of the proton events studied by Cane et al. (1988); all of these speeds are  $>500 \text{ km s}^{-1}$ .

In 19 of the 21 events with clearly associated SEPs, we could observe invariant periods and measure  $e$ -folding decay times ranging from 6 to 18 hr. These timescales are consistent with those expected theoretically (see especially the discussion and appendix in RBN (1996). In the invariant region, we find power-law spectral indices between  $-1.7$  and  $-4.1$  in the 3–11 MeV region; however, many of the spectra steepen at higher energies. Allowing for one event with which a new SEP onset interfered and another that was too small, we are led to conclude that all CME/shock-associated SEP events have periods of spectral invariance. This conclusion is supported in many events that occur before and after the 1979–1982 study period of Sheeley et al. (1985). These include the two events shown in Figures 1–4 and others reported by RBN (1996), the 1995 October event

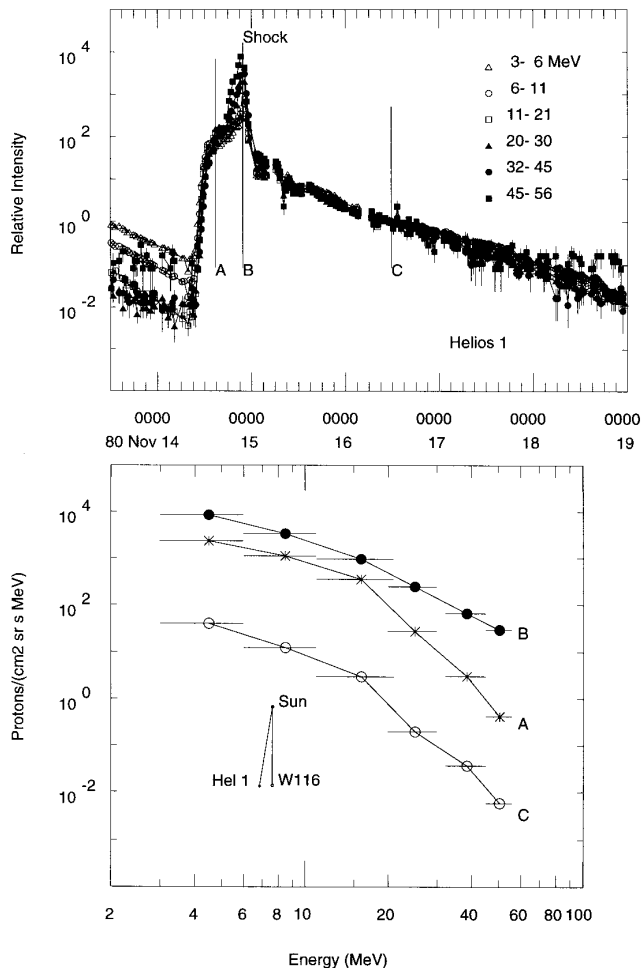


FIG. 6.—Normalized time-intensity profiles for the proton energies shown for *Helios 1* during the 1980 November 14 SEP event. The spacecraft configuration during this event is shown in the inset. Spectra at times A, B, and C in the upper panel are shown in the lower panel. The hardest and most intense spectra occur as the nose of the shock passes over the spacecraft.

TABLE 1  
CME/SHOCK EVENTS AT *HELIOS 1*

Onset Time (UT)	$V_{\text{CME}}$ ( $\text{km s}^{-1}$ )	$\Phi_{\text{CME}}$ (deg)	$V_{\text{avg}}$ ( $\text{km s}^{-1}$ )	$V_{\text{shock}}$ ( $\text{km s}^{-1}$ )	$R_{\text{Hel}}$ (AU)	<i>Helios</i> (deg)	Flare (deg)	Flare- <i>Helios</i> (deg)	3-6 MeV Peak ( $\text{cm}^2 \text{sr s MeV}^{-1}$ )	$T$ (hr)
1979 May 27 (10:44).....	270	55	560	605	0.43	W90	...	...	$390 \pm 39$	6
1979 Jul 3 (01:56).....	590	80	610	$\sim 655$	0.83	W120	...	...	$< 0.009$	...
1979 Oct 10 (07:13).....	170?	50	$\sim 475$	440	0.72	W106	...	...	$< 0.03$	...
1979 Dec 13 (08:19).....	$\sim 350?$	90	460	380	0.55	E77	E16	W61	$< 0.03$	...
1980 Feb 27 (03:27).....	$\geq 600$	60	690	580	0.98	E78	E55	W23	$< 0.04$	...
1980 Mar 2 (22:29).....	...	180	750?	525	0.98	E79	...	...	$< 0.008$	...
1980 Mar 19 (07:06).....	550	60	490	435	0.92	E84	...	...	$< 0.008$	...
1980 Mar 27 (13:58).....	...	47	770	640	0.89	E85	...	...	$40 \pm 4$	...
1980 May 21 (20:51).....	$\sim 420?$	100	590	440	0.34	E24	W15	W39	$2.7 \pm 0.27$	18
1980 Jun 2 (09:00).....	1030	60	570	390	0.33	W42	W93	W51	$7.2 \pm 0.7$	12
1980 Jun 18 (07:57).....	...	80	620	530	0.53	W91	...	...	$5.2 \pm 0.5$	...
1980 Jul 18 (08:42).....	$\sim 400?$	70	545	$\sim 465?$	0.84	W106	...	...	$4.4 \pm 0.4$	12
1980 Jul 29 (12:57).....	$\sim 700?$	50	550	495	0.91	W106	W60	E46	$< 0.09$	...
1980 Nov 14 (06:20).....	$\sim 1100?$	90	$\sim 1510$	1305	0.51	W107	W116	W9	$9200 \pm 920$	15
1981 May 8 (22:21).....	1000	120	970	650	0.67	E95	E37	W58	$360 \pm 36$	7
1981 May 10 (12:08).....	1460	80	1440	$\sim 1330$	0.66	E95	E90	W5	$5600 \pm 560$	14
1981 May 13 (03:28).....	1500	90	1470	1310	0.63	E94	E58	W36	$3200 \pm 320$	9
1981 May 16 (08:06).....	...	360	1790	$\geq 605$	0.59	E93	E14	W79	$3000 \pm 300$	12
1981 Jun 4 (19:27).....	$\sim 700$	70	625	615	0.35	E57	...	...	$29 \pm 3$	18
1981 Jun 18 (09:05).....	1065	30	$\sim 915?$	$\sim 465?$	0.33	W30	W29	E1	$1.4 \pm 0.14$	16
1981 Jul 20 (13:07).....	...	80	870	735	0.72	W90	W75	E15	$5600 \pm 560$	12
1981 Nov 14 (21:53).....	$\geq 550?$	20	680	545	0.67	W79	W49	E30	$5.2 \pm 0.5$	12
1981 Nov 19 (02:29).....	800	50	790	985	0.63	W82	W100	W18	$150 \pm 15$	8
1982 Jan 10 (05:33).....	570	40	455	405	0.54	E110	E90	W20	$< 0.04$	...
1982 Jun 3 (11:41).....	1330	40	1005	840	0.55	E105	E72	W33	$160 \pm 16$	7
1982 Jul 12 (09:06).....	$\geq 700$	200	1030	930	0.44	W50	E37	E87	$2100 \pm 210$	18
1982 Jul 22 (16:34).....	1825	90	1505	$\geq 1200$	0.56	W65	W89	W24	$7800 \pm 780$	16
1982 Dec 7 (23:36).....	$> 1060$	100	1840	$> 1160$	0.59	W67	...	...	$3800 \pm 380$	18
1982 Dec 19 (15:41).....	...	100	900	790	0.44	W91	W75	E16	$15000 \pm 1500$	12

studied by Reames et al. (1997), and also the events of solar cycle 20 shown by McKibben (1972).

## 5. DISCUSSION AND CONCLUSIONS

From the foregoing, we can now identify the region where invariant spectra are seen. For well-connected western SEP events (on the eastern flank of the shock), invariant spectra are seen up to a day before shock arrival and continue through the remainder of the event. For central and eastern SEP events (western flank of the shock), invariance begins after shock passage but usually before the spacecraft passes through the region we associate with the CME itself. Even spacecraft far around on the western flank of the shock eventually see invariant spectra well after shock passage. Once seen, the invariant spectra persist for the remainder of the event when the intensities fall below background or a new onset interferes with it.

The topology of the region of invariant spectra is the region to the left side of the darkened boundary line shown in Figure 7. Here, the magnetic field lines connect to the quasi-parallel region on the eastern flank of the shock. The properties of the shock in this region change only slowly and the regions ahead and, especially, behind the shock can come into equilibrium with the particle population at the shock. This population must itself be declining at least as fast as  $R_{\text{sh}}^{-2}$ , where  $R_{\text{sh}}$  is the radial distance to the shock. Particles are quasi-trapped in the region behind the shock, experiencing intense scattering at the shock and mirroring in the converging fields near the Sun. These particles were originally accelerated at the shock and, in turn, they provide a reservoir or seed population of particles for later acceleration by the shock. In this expanding bottle behind the

shock, adiabatic deceleration, which becomes the primary process for energy change when the shock is several AU beyond the observer, gives the same fractional energy loss at all energies, preserving the spectral shape (RBN 1996). There may also be scattering in the turbulent region in and behind the shock which can lead to cross-field diffusion, after a sufficiently long time, helping to establish similar spectra over the entire region. However, the small spatial

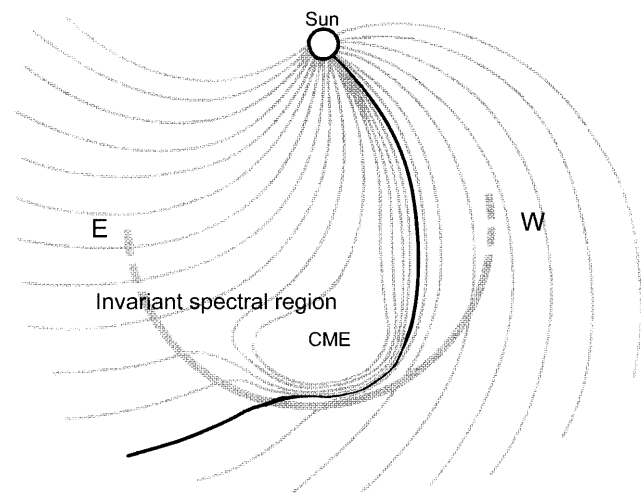


FIG. 7.—The topology leading to invariant spectra is represented by field lines to the left of the darkened boundary in the figure that are connected to the quasi-parallel region on the eastern flank of the shock. Field lines connected to the rapidly varying quasi-perpendicular region on the western flank of the shock usually show harder spectra that vary rapidly in space and time.

scale of intensity fluctuations seen in the *Wind* data for the 1995 October 20 event by Reames et al. (1997) suggest small cross-field diffusion. To the extent that the invariant spectra exist inside the CME, particles must have entered the region through reconnected field lines (see, e.g., Gosling, Birn, & Hesse 1995).

In the region on the right-hand side of Figure 7, the situation is much more dynamic. Consider a single field line or flux tube to the west of the source. When the western flank of the shock first intercepts this field line, it is quasi-perpendicular to it and  $\theta_{Bn}$ , the angle between the field direction and shock normal, then changes continuously as the shock sweeps out the field line. Different portions of the shock surface, perhaps with different speeds, intercept this field line at different times. Particles trapped on this field line are accelerated and reaccelerated as they reencounter the shock. In addition, the spacecraft crosses from one field line to another, exaggerating these differences, as its connection longitude to the shock sweeps eastward across the face of the shock with time. In the quasi-perpendicular region,

low-energy particles have difficulty overtaking the shock and are swept behind it, while high-energy particles are more efficiently accelerated. This selective and efficient re-processing of high-energy particles leads to spectra that are harder than those in the invariant region. A spacecraft that crosses the quasi-perpendicular shock will very quickly have its magnetic connection swept toward the nose of the shock and find itself connected to the quasi-parallel region with its softer, invariant spectra. In many cases, the boundary that marks the onset of the invariant region seems quite sharp because of field compression; we have shown it as a heavy line in Figure 7.

Our statistical study of the events in the Sheeley et al. (1985) list confirms the evidence from representative events seen on many different spacecraft before and after the 1979–1982 period that Sheeley et al. (1985) studied. This evidence strongly suggests that invariant spectra are a common feature caused by the evolving topology of a well-defined spatial region that occurs in all gradual SEP events.

#### REFERENCES

- Cane, H. V., McGuire, R. E., & von Rosenvinge, T. T. 1986, *ApJ*, 301, 448  
 Cane, H. V., Reames, D. V., & von Rosenvinge, T. T. 1988, *J. Geophys. Res.*, 93, 9555  
 Gosling, J. T. 1993, *J. Geophys. Res.*, 98, 18,949  
 Gosling, J. T., Birn, J., & Hesse, M. 1995, *Geophys. Res. Lett.*, 22, 869  
 Kahler, S. W. 1992, *ARA&A*, 30, 113  
 ———. 1994, *ApJ*, 428, 837  
 Kahler, S. W., Cliver, E. W., Cane, H. V., McGuire, R. E., Reames, D. V., Sheeley, N. R., Jr., & Howard, R. A. 1987, in *Proc. 20th Int. Cosmic-Ray Conf. (Moscow)*, 3, 121  
 Kahler, S. W., Sheeley, N. R., Jr., Howard, R. A., Koomen, M. J., Michels, D. J., McGuire, R. E., von Rosenvinge, T. T., & Reames, D. V. 1984, *J. Geophys. Res.*, 89, 9683  
 Leske, R. A., Cummings, J. R., Mewaldt, R. A., Stone, E. C., & von Rosenvinge, T. T. 1995, *ApJ*, 452, L149  
 Luhn, A., Klecker, B., Hovestadt, D., Gloeckler, G., Ipavich, F. M., Scholer, M., Fan, C. Y., & Fisk, L. A. 1984, *Adv. Space Res.*, 4(2), 161  
 Luhn, A., Klecker, B., Hovestadt, D., & Mobius, E. 1987, *ApJ*, 317, 951  
 Mason, G. M., Gloeckler, G., & Hovestadt, D. 1984, *ApJ*, 280, 902  
 Mason, G. M., Mazur, J. E.,Looper, M. D., & Mewaldt, R. A. 1995, *ApJ*, 452, 901  
 McKibben, R. B. 1972, *J. Geophys. Res.*, 77, 3959  
 Oetliker, M., et al. 1997, *ApJ*, 477, 495  
 Reames, D. V. 1990, *ApJS*, 73, 235  
 ———. 1993, *Adv. Space Res.*, 13(9), 331  
 ———. 1995a, *Rev. Geophys. Suppl.*, 33, 585  
 ———. 1995b, *Adv. Space Res.*, 15(7), 41  
 Reames, D. V., Barbier, L. M., & Ng, C. K. 1996, *ApJ*, 466, 473 (RBN)  
 Reames, D. V., Barbier, L. M., von Rosenvinge, T. T., Mason, G. M., Mazur, J. E., & Dwyer, J. R. 1997, *ApJ*, 483, 515  
 Reames, D. V., & Stone, R. G. 1986, *ApJ*, 308, 902  
 Sheeley, N. R., Jr., Howard, R. A., Koomen, M. J., Michels, D. J., Schwenn, R., Mühlhäuser, K. H., & Rosenbauer, H. 1985, *J. Geophys. Res.*, 90, 163  
 Tylka, A. J., Boberg, P. R., Adams, J. H., Jr., Beahm, L. P., Dietrich, W. F., & Kleis, T. 1995, *ApJ*, 444, L109